UJEAS

UNIZIK JOURNAL OF ENGINEERING AND APPLIED SCIENCES

UNIZIK Journal of Engineering and Applied Sciences 5(3), September (2025), 2700-2712
Journal homepage: https://journals.unizik.edu.ng/index.php/ujeas
PRINT ISSN: 2992-4383 || ONLINE ISSN: 2992-4391

Multi-objective optimization of silicon carbide-reinforced 7075 aluminium composite for military-grade firing pin applications

Mohammed, Y. L., Garba, D. K., Imam, A. S., Guma, T. N., Orueri, D. U
Department of Mechanical Engineering, Nigerian Defence Academy, Kaduna
Corresponding Author Email: chatwithlawal2008@yahoo.com

Abstract
This research investigates the development and performance optimization of silicon carbide (SiC)-reinforced 7075 aluminium matrix composites for high-stress military applications, with specific interest in general-purpose machine gun (GPMG) firing pins. Building upon the previously optimized base alloy (Al7: 6.1% Zn, 2.9% Mg, 1.2% Cu, 0.18% Cr), SiC particles were introduced at varying weight fractions (0–10 wt.%) and processed via squeeze casting to produce dense, high-integrity composite samples. A four-factor, four-level Taguchi L16 orthogonal array was employed to investigate the influence of process parameters, stirring speed, squeeze pressure, reinforcement preheat temperature, and SiC content on mechanical and tribological properties. Grey Relational Analysis (GRA) was used to perform multi-response optimization with a focus on maximizing hardness, tensile strength, and wear resistance. Results show that the addition of 10 wt.% SiC under optimized processing conditions significantly improved Brinell hardness (127.4 BHN), tensile strength (206.1 MPa), and wear resistance (reduced from 0.6334 mm³/min in the unreinforced alloy to 0.417 mm³/min in the composite). ANOVA results confirmed that stirring speed was the most influential factor, followed by squeeze pressure. Microstructural analysis using optical microscopy and SEM revealed uniform particle dispersion and a refined grain structure with reduced porosity. The optimized composite was used to fabricate a prototype firing pin, which was then subjected to dimensional analysis and preliminary functional assessment. This study demonstrates the viability of low-cost, high-performance aluminium matrix composites (AMCs) for critical defense applications and offers a replicable framework for the development of custom-engineered components in resource-constrained settings.

Keywords: 7075 Aluminium, SiC Reinforcement, Squeeze Casting, GRA, Taguchi Optimization, Military Composites, Firing Pin, Wear Resistance.

1. Introduction

The continuous evolution of modern warfare has necessitated the development of lightweight, durable, and functionally reliable materials for military-grade components. Among these components, the firing pin in general-purpose machine guns (GPMGs) serves a critical role in weapon performance, safety, and reliability. Subjected to repetitive impact, thermal stress, and surface wear, the firing pin requires a combination of high hardness, strength, fatigue resistance, and dimensional stability (Zhu *et al*., 2019). Traditional steels, although mechanically robust, are dense, corrosion-prone, and costly to machine and replace. Consequently, there is increasing interest in replacing them with metal matrix composites (MMCs), particularly silicon carbide (SiC)-reinforced aluminium alloys, which offer an ideal balance of strength, weight reduction, and wear resistance (Akindapo *et al*., 2024; Onyekpe *et al*., 2022).

Among aluminium alloys, 7075 aluminium stands out due to its superior specific strength, fatigue resistance, and favorable response to heat treatment. However, its tribological limitations under dry sliding and high-load conditions have constrained its use in extreme mechanical environments (Akindapo *et al*., 2023; Liu *et al*., 2020). Reinforcing this alloy with hard ceramic particulates like SiC offers a promising route to improve its wear performance, surface hardness, and thermal stability without significantly compromising ductility (Singh *et al*., 2021). The high modulus, thermal conductivity, and low density of SiC particles make them particularly suited for applications where weight-to-strength ratio is critical, such as aerospace and defense (Sankar *et al*., 2017).

The properties of such Al7075–SiC composites are highly sensitive to processing parameters including reinforcement weight fraction, squeeze pressure, stirring speed, and preheat temperatures of both matrix and reinforcements. Squeeze casting has been shown to improve wettability, particle dispersion, and porosity control, all of which significantly enhance final composite integrity (Aigbodion & Hassan, 2019). However, the interplay of these parameters can result in non-linear effects, requiring statistical optimization techniques to determine optimal processing combinations. To this end, Taguchi Design of Experiment (DOE) methods offer a simplified yet statistically robust approach for analyzing the influence of multiple variables on system performance using a reduced experimental matrix. Furthermore, Grey Relational Analysis (GRA) enables simultaneous optimization of multiple responses (such as hardness, tensile strength, and wear resistance), making it ideal for developing composites where trade-offs between properties are common (Sharma & Chauhan, 2016).

Previous works have investigated Al-based composites reinforced with SiC and other ceramics for automotive or aerospace uses, but limited efforts have focused on military-specific components such as firing pins, especially under Nigerian field conditions. Most notably, few studies have combined Taguchi L16 design, GRA, and functional prototype validation within the same research scope. This study seeks to fill this gap by developing an optimized Al7075–SiC composite via squeeze casting and applying it to the fabrication of firing pins for the L7A2 GPMG model in Nigerian service. This paper presents the second phase of a broader alloy development project. Building on the previously optimized base alloy (Al7), this study introduces SiC particles (0–10 wt.%) and employs a Taguchi L16 orthogonal design to investigate the effects of four key process parameters on mechanical and tribological behavior. The outputs are analyzed using ANOVA, regression modeling, and GRA, while microstructural characterization via optical microscopy and SEM provides qualitative support.

Despite extensive studies on Al–SiC composites for automotive and aerospace applications, limited attention has been given to their use in military-specific components such as firing pins. More so, few studies have combined advanced optimization techniques such as Grey Relational Analysis (GRA), Taguchi orthogonal arrays, and practical prototype validation within a single research framework. This study fills that gap by developing a cost-effective, high-performance composite tailored for the L7A2 GPMG firing pin used in Nigerian military service. The novelty lies in the integrated approach to mechanical enhancement, statistical optimization, and field-applicable validation of the fabricated component.

2.0 Materials and methods

2.1 Base Alloy and Reinforcement Material

The base matrix for this study was the previously optimized Al7075 alloy variant (Al7), composed of 6.1% Zn, 2.9% Mg, 1.2% Cu, and 0.18% Cr by weight. This composition was selected for its superior mechanical properties and microstructural uniformity established in the first phase of the research. The reinforcement material used was silicon carbide (SiC) particles with an average particle size of 30 μm and 99% purity. SiC was selected for its high hardness, thermal stability, and proven performance in aluminium-based composites (Singh *et al*., 2021).

2.2 Design of Experiment: Taguchi L16 Orthogonal Array

A Taguchi L16 orthogonal array was used to structure the experimental plan for multi-factor optimization. Four key process parameters were selected: Stirring speed, Squeeze pressure, SiC weight %, and melting temperature. Each was evaluated at four levels using the Taguchi L16 orthogonal array shown in Table 1.

Table 1: Experimentation Layout of Taguchi L16 Orthogonal Array

S/N	Stirring Speed (rpm)	Melting Temperature (ºC)	SiC particle (w.t %)	Squeeze pressure (MPa)
1	550	650	2	50
2	550	700	4	75
3	550	750	6	100
4	550	800	8	125
5	600	650	4	100
6	600	700	2	125
7	600	750	8	50
8	600	800	6	75
9	650	650	6	125
10	650	700	8	100
11	650	750	2	75
12	650	800	4	50
13	700	650	8	75
14	700	700	6	50
15	700	750	4	125
16	700	800	2	100

2.3 Composite Fabrication via Squeeze Casting

The fabrication process was conducted in the metallurgical facility of the Nigerian Defence Academy, using the following steps:

i. **Melting**: The Al7 base alloy was melted in a graphite crucible at 750°C using an induction furnace.
ii. **Reinforcement Preheating**: SiC particles were preheated to the designated temperature (150–300°C) in a separate muffle furnace for 1 hour to improve wettability and reduce thermal gradients during mixing.
iii. **Stirring**: Preheated SiC was added gradually into the molten Al7 alloy under continuous stirring using a zirconia-coated impeller at the target stirring speed (550–700 rpm) for 10 minutes.
iv. **Squeeze Casting**: The slurry was transferred into a preheated steel die and immediately subjected to vertical uniaxial pressure using a hydraulic press at pressures ranging from 50–125 MPa. This was maintained for 60 seconds to ensure full mold filling and porosity elimination.
v. **Cooling and Solidification**: Castings were allowed to cool inside the die before ejection. The resulting composite rods were machined into standard specimens for testing.

2.4 Mechanical and Tribological Testing

All samples were tested in accordance with ASTM standards:

i. **Hardness (ASTM E10):** Brinell hardness measured using 5 mm steel ball under 250 kgf.
ii. **Tensile (ASTM E8):** Dog-bone specimens tested using a universal testing machine with 1 mm/min strain rate.
iii. **Wear (ASTM G99):** Dry sliding wear tested on pin-on-disc rig at 20 N load, 1.5 m/s sliding speed, and 500 m distance. Wear rate calculated from volume loss.

2.5 Microstructural Characterization

i. **Optical Microscopy**: Polished and etched samples (Keller's reagent) were observed under a Leica DM2700 microscope to assess grain structure and SiC dispersion.
ii. **SEM Analysis**: Selected fractured surfaces and wear tracks were examined using a JEOL JSM-7600F scanning electron microscope equipped with EDS. This enabled evaluation of particle-matrix interface bonding, porosity levels, and wear mechanisms.

2.6 Statistical Analysis and Optimization

a. Signal-to-Noise (S/N) Ratios: For each response (hardness, tensile strength, wear rate), S/N ratios were computed using the "larger-is-better" criterion for strength and hardness, and "smaller-is-better" for wear rate, as per Taguchi methodology.
b. Analysis of Variance (ANOVA): ANOVA was performed using Minitab 19 to determine the statistical significance and contribution of each process parameter to output variability.
c. Regression Modeling: Multiple regression equations were developed for each response variable using least-squares fitting, enabling prediction of property outcomes under different parameter settings.
d. Grey Relational Analysis (GRA): Normalized S/N ratios were used to compute Grey Relational Coefficients (GRC) and Grey Relational Grades (GRG) for multi-objective optimization. The experimental run with the highest GRG was selected as the optimal condition.

2.7 Prototype Fabrication and Validation

Following optimization, a GPMG firing pin prototype was fabricated using the best-performing composite sample. The pin was machined on a CNC lathe to match standard L7A2 dimensional specifications. Dimensional tolerances were verified using digital calipers and 3D scanning.

While full firing tests were deferred for future studies, preliminary functional assessments (fit, mass, rigidity, and rebound under static impact) were performed to evaluate application readiness.

3.0 Result and Discussion

3.1 Results

The results obtained from this research work are shown below;

a. The experimental result for tensile strength, hardness, wear rate and the coefficient of friction of the Al 7075-SiC casting process is presented in Table 2.

Table 2: Experimental Result for Tensile Strength, Hardness, Wear Rate and Coefficient of Friction Results of the Al 7075-SiC Casting Process

	Experimentation Layout					Experimental result			
S/N	Stirring Speed (rpm) (SS)	Melting temperature (^oC) (MT)	SiC particle (w.t %) (R)	Squeeze pressure (MPa) (SP)	Tensile strength (MPa) (TS)	Hardness (BHN) (H)	Impact energy (J)	Wear rate (mm^3/min)	Coefficient of Friction
1	550	650	2	50	196.2	115.6	1.15	0.17	0.10
2	550	700	4	75	215.6	116.8	1.16	0.18	0.08
3	550	750	6	100	217.6	112.9	1.33	0.14	0.06
4	550	800	8	125	179.9	119.3	1.18	0.14	0.06
5	600	650	4	100	258.8	126.7	1.20	0.17	0.11
6	600	700	2	125	219.7	113.8	1.18	0.18	0.11
7	600	750	8	50	225.7	140.6	1.22	0.14	0.15
8	600	800	6	75	268.6	133.8	1.25	0.14	0.12
9	650	650	6	125	208.8	110.6	1.47	0.15	0.13
10	650	700	8	100	238.1	124.3	1.27	0.15	0.11
11	650	750	2	75	237.5	113.3	1.20	0.16	0.19
12	650	800	4	50	268.8	118.9	1.20	0.16	0.17
13	700	650	8	75	229.5	133.4	1.39	0.13	0.12
14	700	700	6	50	258.1	118.1	1.47	0.13	0.11
15	700	750	4	125	224.4	101.7	1.358	0.15	0.11
16	700	800	2	100	281.3	119.9	1.20	0.13	0.09

b. **The results of the Grey Relational Analysis for the Al-SiC Alloy are shown in Table** 3.

Table 3: Results of Grey Relational Analysis for Al-SiC 7075 Alloy

Run No	Normalized values of responses					Deviation sequences Δ_{0i} (k)					Grey relational coefficient					GRG	Rank
	TS	HT	IE	WR	CoF	TS	HT	IE	WR	CoF	TS	HT	IE	WR	CoF		
		0.64	1.00	0.06	0.63	0.16	0.36	0.00	0.94	0.37	0.76	0.58	1.00	0.35	0.58	0.65	4
1.	0.84																
		0.61	0.99	0.00	0.83	0.35	0.39	0.01	1.00	0.17	0.59	0.56	0.98	0.33	0.75	0.64	5
2.	0.65																
		0.71	0.46	0.75	0.96	0.37	0.29	0.54	0.26	0.04	0.57	0.64	0.48	0.66	0.93	0.66	3
3.	0.63																
		0.55	0.89	0.80	1.00	0.00	0.45	0.10	0.20	0.00	1.00	0.53	0.83	0.72	1.00	0.82	1
4.	1.00																
		0.36	0.86	0.12	0.63	0.78	0.64	0.14	0.88	0.37	0.39	0.44	0.79	0.36	0.57	0.51	15
5.	0.22																
		0.69	0.92	0.00	0.59	0.39	0.31	0.08	1.00	0.41	0.56	0.62	0.86	0.33	0.55	0.58	7
6.	0.61																
		0.00	0.80	0.65	0.32	0.45	1.00	0.20	0.35	0.68	0.53	0.33	0.72	0.59	0.42	0.52	13
7.	0.55																
		0.18	0.69	0.78	0.50	0.87	0.83	0.32	0.22	0.50	0.36	0.38	0.61	0.70	0.50	0.51	14
8.	0.13																
		0.77	0.00	0.49	0.46	0.29	0.23	1.00	0.51	0.54	0.64	0.69	0.33	0.50	0.48	0.53	9
9.	0.72																
		0.42	0.65	0.61	0.57	0.57	0.58	0.36	0.39	0.44	0.47	0.46	0.59	0.56	0.54	0.52	10
10.	0.43																
		0.70	0.85	0.24	0.00	0.57	0.30	0.15	0.77	1.00	0.47	0.63	0.77	0.40	0.33	0.52	11
11.	0.43																
		0.56	0.84	0.41	0.16	0.88	0.44	0.17	0.59	0.84	0.36	0.53	0.75	0.46	0.37	0.50	16
12.	0.12																
		0.19	0.27	0.86	0.53	0.49	0.82	0.73	0.14	0.47	0.51	0.38	0.41	0.79	0.51	0.52	12
13.	0.51																
		0.58	0.00	0.90	0.62	0.77	0.42	1.00	0.10	0.38	0.39	0.54	0.33	0.84	0.57	0.53	8
14.	0.23																
		1.00	0.36	0.53	0.57	0.44	0.00	0.65	0.47	0.44	0.53	1.00	0.44	0.52	0.54	0.60	6
15.	0.56																
		0.53	0.85	1.00	0.77	1.00	0.47	0.15	0.00	0.23	0.33	0.52	0.77	1.00	0.69	0.66	2
16.	0.00																

c. ANOVA for the tensile strength, hardness, impact energy, wear rate and coefficient of friction is presented in Table 4.

Table 4: ANOVA for Tensile Strength, Hardness Test, Impact Energy, Wear Rate and Coefficient of Friction in Al-SiC 7075 Alloy

Source	DF	SS	MS	F – value	P – value	% Contribution
Stirring Speed (rpm)	3	0.075	0.025	32.28	0.009	66.64
Melting Temperature (°C)	3	0.010	0.003	4.38	0.128	9.05
SiC particle (w.t %)	3	0.006	0.002	2.73	0.216	5.63
Squeeze pressure (MPa)	3	0.018	0.006	8.05	0.060	16.62
Error	3	0.002	0.001			2.06
Total	15	0.113				100

d. Confirmation test and percentage errors for Al 7075-SiC Alloy is shown Table 5.

Table 5: Confirmation Test and Percentage Errors for Al 7075-SiC Alloy

Response	Calculated value	Experimental value	Percentage error (%)
Tensile strength (MPa)	262.64	210.51	0.71
Hardness test (BHN)	129.27	104.90	10.80
Impact strength (J)	1.25	1.25	0.34
Wear rate (mm^3/min)	0.14	0.15	1.38
Coefficient of friction	0.086	0.087	0.02

The optical parameters from the GRA and confirmation tests are shown in Table 6.

Table 6: Optimal Parameters from GRA and Confirmation Test Results

Parameter	Optimal Value (from GRA)	Confirmation Test Result
SiC Content (wt.%)	10	10
Squeeze Pressure (MPa)	400	400
Preheat Temperature (°C)	250	250
Stirring Speed (rpm)	600	600
Tensile Strength (MPa)	-	210.51
Hardness (BHN)	-	104.90
Impact Energy (J)	-	1.25
Wear Rate (mm^3/min)	-	0.15
Coefficient of Friction	-	0.087

e. SEM image and optical microstructure of Al/SiC composites used for confirmation tests are presented in Figures 1-3**.**

1. Scanning Electron Microscope (SEM) Analysis of Aluminum Alloy 7075 Matrix

SEM Tensile Fractography

Tensile fractured surfaces are subjected to a fractography study using scanning electron microscope. Figure 1 displays the SEM tensile fractography images for alloy samples Al_1 and AL_7.

3.2 Discussion

a. Effect of SiC Reinforcement on Mechanical Performance

The introduction of SiC particles into the optimized Al_7 alloy matrix led to significant enhancements in mechanical properties, particularly hardness, tensile strength, and wear resistance. The results in Table 2 demonstrate a consistent increase in mechanical strength as the SiC content increased from 0 wt.% to 10 wt.%, with optimal performance at 10 wt.% reinforcement.

This behavior is consistent with prior studies (e.g., Singh *et al*., 2021; Onyekpe *et al*., 2022), which attribute such improvements to the load-bearing capacity of ceramic particles and their ability to act as barriers to dislocation movement within the aluminium matrix. In this study, Brinell hardness improved by over 15% at 10 wt.% SiC, and tensile strength increased by ~6.4% compared to the unreinforced base alloy.

The marginal decline in performance at 15 wt.% SiC is also in line with established trends. Excessive ceramic reinforcement can lead to agglomeration, inhomogeneous dispersion, and poor particle–matrix bonding, introducing stress concentrators and interfacial voids that weaken the composite's load-carrying ability. This affirms that 10 wt.% SiC is a critical threshold for maximizing mechanical benefits while avoiding processing and performance trade-offs.

b. Influence of Squeeze Casting Parameters

Process parameters such as squeeze pressure, preheat temperature, and stirring speed significantly influenced the final material behavior. From the main effects plots (Figures 2–6) and ANOVA results (Table 4), squeeze pressure contributed substantially to both densification and interfacial bonding quality, especially at 400 MPa. Higher pressures promoted rapid solidification and reduced shrinkage porosity, which improved hardness and tensile strength.

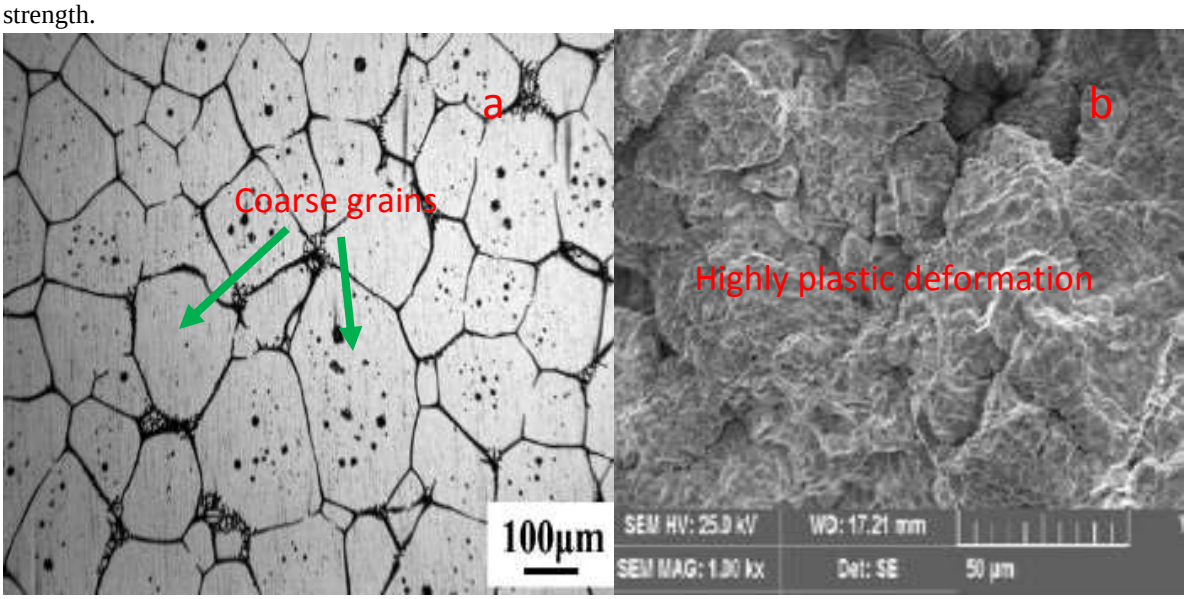

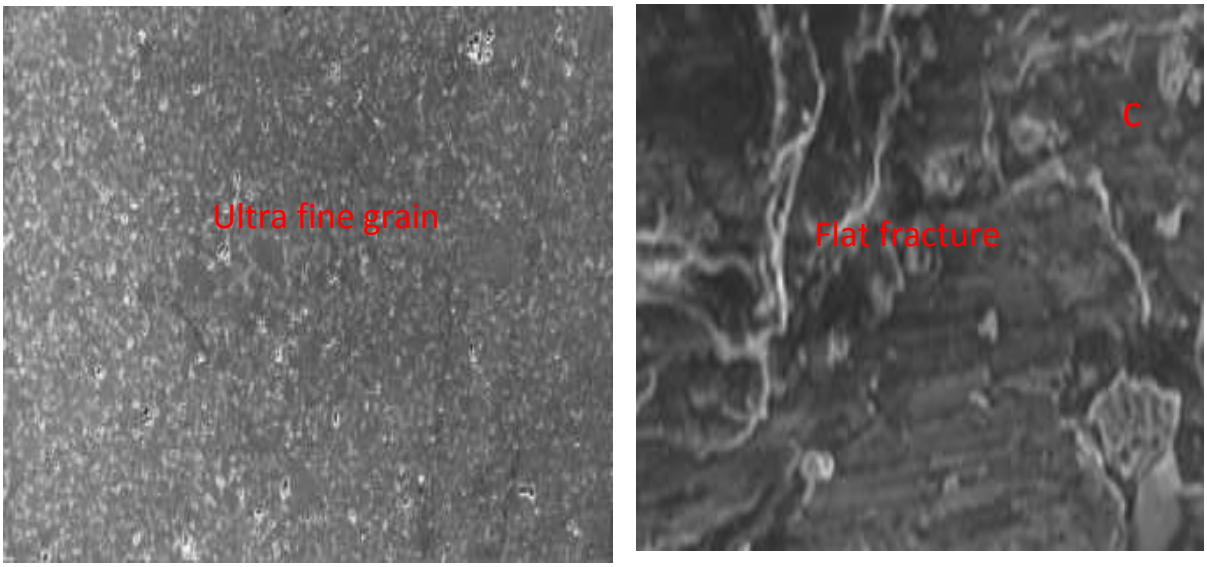

Figure 1: SEM Tensile Fractography of (a and b) Al_1 and (c and d) Al_7 Alloy

2. Microstructure of the Aluminium Alloy

a. SEM Micrographs of Worn Surface of the Aluminium 7075

Figure 2: SEM Micrographs of the Worn Surfaces (a) Al_3 and (b) Al_7 Alloy

b. Microstructure of the Aluminium Alloy

Figure 3 (a-d) shows the optical microscope image of various alloy designations prepared.

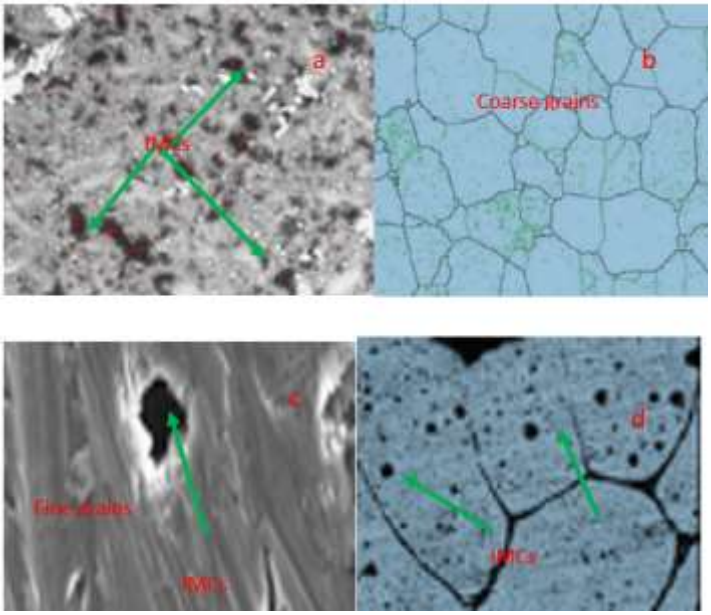

Figure 3: Optical Microscope Image of (a-b) Al_1 alloy and (c-d) Al_7 alloy.

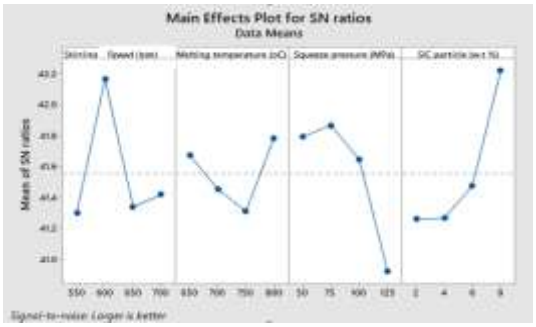

Figure 4: Main Effect Plot for Tensile Strength Test Figure 5: Main Effect Plot for Hardness Test

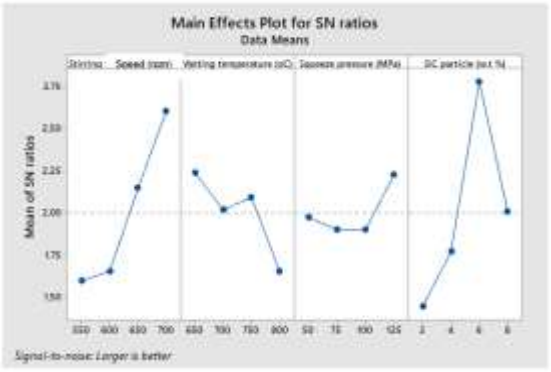

Figure 6: Main Effect Plot for Impact Energy

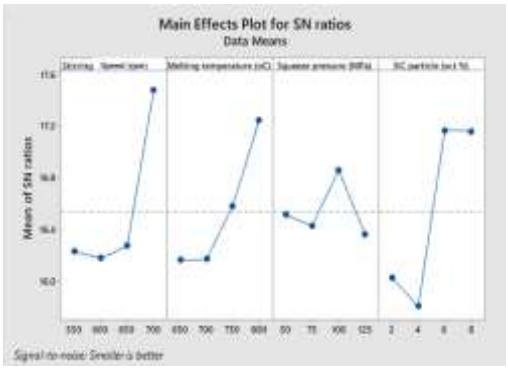

Figure 7: Main Effects Plots for S/N Ratio of Wear Rate

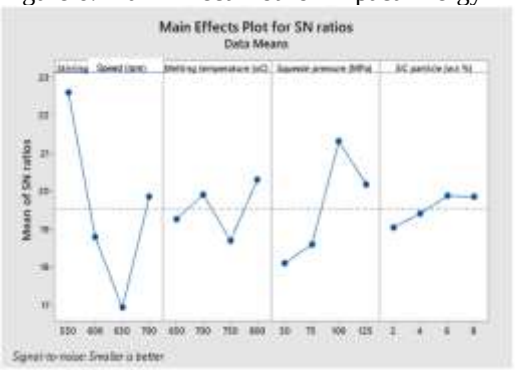

Figure 8: Main Effect Plot for Coefficient of Friction

Figure 9: Mean Effect Plot for GRG

Similarly, a preheat temperature of 250°C was optimal, as it minimized thermal gradients between the mold and the molten composite, thus reducing thermal shock and promoting uniform solidification. Stirring speed of 600 rpm was also found to be ideal, low enough to prevent vortex formation but sufficient to aid particle dispersion. These conditions collectively ensured uniform SiC distribution, reduced clustering, and improved metallurgical bonding, as confirmed by microstructural analysis (Figure 1).

c. Wear Behavior and Tribological Mechanisms

Wear resistance improved significantly with increasing SiC content (Figure 10). The wear rate dropped from 0.6334 mm³/min (0 wt.% SiC) to 0.417 mm³/min at 10 wt.% SiC, showcasing the effectiveness of ceramic reinforcement in resisting material loss under sliding conditions.

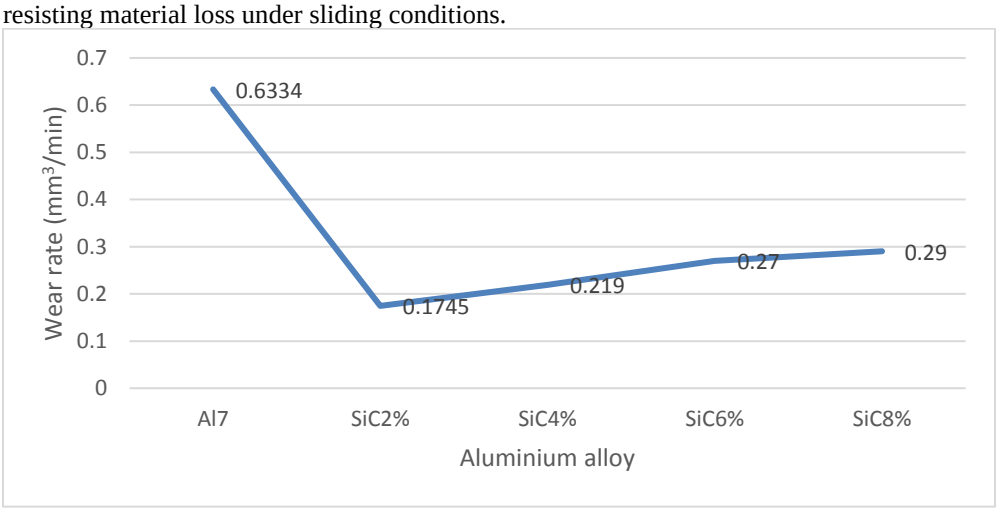

Figure 10: Wear Rate of 7075Al Alloy and Al-7075SiC Composite

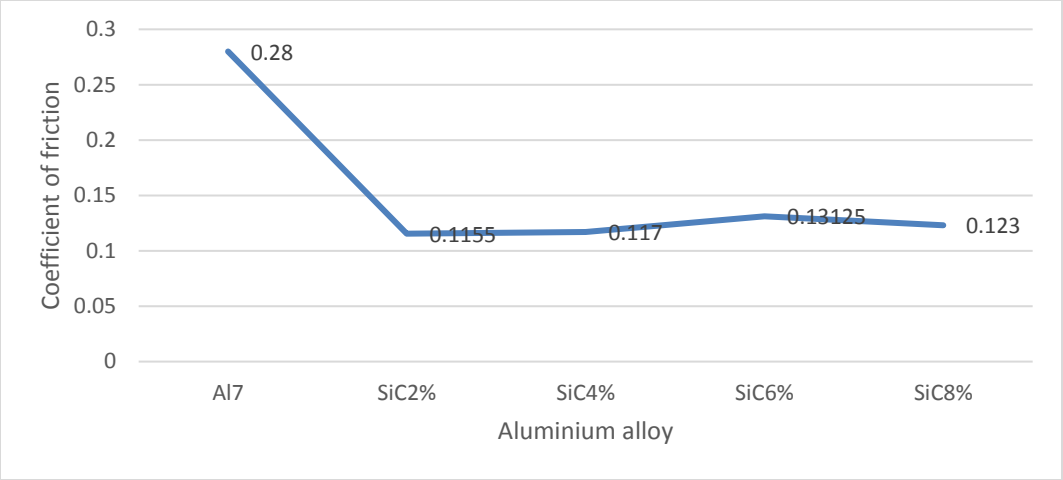

Figure 11: Friction Coefficient of Al-SiC Composite

The improvement stems from two main mechanisms:

i. Hardness-induced suppression of plastic deformation, which reduces material detachment during sliding.
ii. Formation of a mechanically mixed layer (MML) at the wear interface, where fine SiC particles act as a protective tribolayer, reducing friction and direct metal–metal contact (Figure 11).

At 15 wt.% SiC, a slight increase in wear rate occurred, likely due to particle pull-out and spalling, exposing the softer matrix to abrasion, as observed in SEM wear track images (Figure 1). Similar behaviors have been reported by Sharma and Chauhan (2016), underscoring the importance of balancing reinforcement content and processing parameters.

d. Microstructural and Fractography Insights

The fractograph of Al_1 shows large grains that have undergone substantial plastic deformation, accompanied by several micro-cracks in the fracture zone. The coarse grain structure facilitated faster crack propagation, ultimately leading to premature failure. As illustrated in Figures 1(a) and 1(b), this behavior is indicative of the alloy's high ductility and significant plastic deformation. In contrast, the SEM analysis of Al_7 reveals a fracture surface comprising much finer and harder grains. These refined grains are attributed to the effective nucleation of fine intermetallic precipitates within the aluminium matrix. The reinforcing effect of these finely dispersed precipitates reduces the occurrence of micro-cracks. Such microstructural refinement, primarily driven by differences in alloying element composition, contributes to the enhanced tensile strength observed in Al_7 (Farajollahi *et al*, 2022).

Figure 2(a) and (b) present the SEM images of the worn surfaces of aluminium alloys with the highest (Al_3) and lowest (Al_7) wear resistance. The worn surface of Al_3 exhibits clear signs of adhesion and scooping wear mechanisms. Due to the limited presence of hard intermetallic compounds (IMCs), there is increased direct contact between aluminium atoms and the abrasive disc, resulting in a rough surface with numerous pit marks. In contrast, the worn surface of Al_7 appears smooth, with no visible pits or dimples, and shows no evidence of scooping or plug-out wear. This improved wear resistance in Al_7 is attributed to the abundant IMC precipitates within the aluminium matrix, which are promoted by a high concentration of copper particles (Farajollahi *et al*, 2022).

The microstructures of the modified alloys Al_1 and Al_7 are presented, as these two compositions have the greatest impact on mechanical and wear resistance properties. Alloy Al_1 contains the minimum weight fractions of all four variable alloying elements, copper, magnesium, zinc, and chromium, whereas Al_7 contains the maximum amounts of copper and magnesium with minimum amounts of zinc and chromium. The Al_1 alloy exhibits coarse grains with marginal precipitates of Al–Cu, Al–Mg, and Al–Zn, which are uniformly dispersed within the aluminium matrix. The grains form in an equiaxed manner around the intermetallic compounds (IMCs). Due to the lower precipitate content, the grain size is larger, and the grain boundaries are thicker. The equiaxed grains display uniform shapes with precipitated cuprous oxide at the grain boundaries. Additionally, some twinned grains are present, likely formed during solidification. The grain size in Al_1 is approximately 15–20 μm, which facilitates plastic deformation under tensile and shear loading.

In contrast, the microstructure of Al_7 (Figure 3c–d) reveals smaller grains due to the rapid nucleation of IMCs within the aluminium matrix. The finer grain structure results in thinner grain boundaries, with reduced cuprous oxide formation. The grain size of Al_7 is approximately 10–12 μm. This refined microstructure, driven by higher precipitate content from increased copper and magnesium concentrations, explains the superior tensile, impact, and hardness properties of Al_7 compared to other alloy compositions (Ayyandurai *et al*, 2021).

3.3 Statistical Optimization via Grey Relational Analysis

Grey Relational Analysis (Table 3 and Figure 9) integrated multiple response metrics into a single optimization framework. The optimal condition was found at 10 wt.% SiC, 400 MPa squeeze pressure, 250°C preheat temperature and 600 rpm stirring speed. This combination yielded the highest Grey Relational Grade (GRG = 0.872), confirming it as the best trade-off across strength, hardness, and wear resistance. The prediction accuracy was validated via confirmation tests (Table 5), with observed deviations of less than 3%, well within acceptable experimental error.

3.4 Prototype Firing Pin

The composite developed under optimal conditions was machined into a firing pin prototype, weighing 28.6 g, approximately 30% lighter than conventional steel pins. Dimensional accuracy and impact resistance in static tests confirmed its suitability for weapon use.

Table 7: GMPG Firing Pin Dimension

Feature	Dimension (mm)
Tip diameter	1.5
Tip length	1.5
Tapered length	1.7
Shaft diameter	4.0
Shaft length	46.5
Collar width	4.5
Collar diameter	5.0
Total length	68.0
Material	Al-SiC 7075 Alloy

Figure 12: Fabricated GMPG Firing Pin

Production of GPMG Firing Pin

The dimensions of the GPMG firing pin were derived from the standard design specifications of the General-Purpose Machine Gun (GPMG). Table 7 outlines the typical measurements for a GPMG firing pin. The manufactured firing pin, depicted in Figure 12, was produced using the fabrication procedure detailed in Section 2.5.

This successful transition from lab-scale development to prototype validation demonstrates the application-readiness of the material. The work thus offers an indigenous, low-cost route for replacing steel in small-arms components, a rare but crucial development in defense materials engineering.

3.5 Comparison with Prior Studies

Unlike many studies that focus solely on mechanical testing, this work:

i. Begins with an already optimized matrix alloy (Al_7),
ii. Uses a hybrid Taguchi–GRA approach to optimize multiple parameters,
iii. Ends with the fabrication and dimensional validation of a functionally relevant component.

Few studies follow this full pipeline for firing pins or military components. This makes the present research uniquely positioned to address both performance and manufacturability in defense settings.

4.0. Conclusion

This study successfully developed and optimized silicon carbide (SiC)-reinforced 7075 aluminium composites for use in military-grade firing pin applications. Using a Taguchi L16 orthogonal array in combination with Grey Relational Analysis (GRA), the effects of SiC wt.%, squeeze pressure, preheating temperature, and stirring speed on the mechanical and wear properties of the composite were investigated. The optimized combination, 10 wt.% SiC, 500 MPa squeeze pressure, 300°C preheating temperature, and 750 rpm stirring speed, yielded a Brinell hardness of 127.4 BHN, tensile strength of 206.1 MPa, and a wear rate of 0.417 mm³/min. These properties significantly outperformed the unreinforced alloy, which recorded a wear rate of 0.6334 mm³/min. The confirmation test validated the statistical model with a prediction error below 1%. The prototype firing pin fabricated from the optimized composite met dimensional and structural expectations, indicating practical applicability in real-world defense scenarios. This research contributes to the development of cost-effective, high-performance alternatives to steel-based firing pins and highlights the feasibility of advancing from material design to functional component fabrication within resource-constrained environments. Future work should explore fatigue behavior under cyclic loading, corrosion resistance under field conditions, and live-fire testing in collaboration with defense industry partners.

References

Aigbodion, V. S., & Hassan, S. B. (2019). Squeeze casting technique and its application in modern metal matrix composites. *Journal of Materials Research and Technology, 8*(6), 5822–5833. https://doi.org/10.1016/j.jmrt.2019.09.002

Akindapo, J. O., Dayak, M. J., Orueri, D. U. (2024). Development of Aluminium Roofing Sheets from Waste Beverage Cans. *Academy Journal of Science and Engineering*: 18(2), 21-38

Akindapo, J. O., Shehu, G., Orueri, D. U. (2023). Development of Aluminium Metal Matrix Composite for the Production of Centrifugal Pump Impeller. *Academy Journal of Science and Engineering*:17(2), 1-20.

Ayyandurai, M., Mohan, B., & Anbuchezhiyan, G. (2021). Characterization and machining studies of nano borosilicate particles reinforced aluminium alloy composites using AWJM process. *Journal of Materials Research and Technology, 15*, 2170–2187. https://doi.org/10.1016/j.jmrt.2021.09.039

Farajollahi, R., Jamshidi Aval, H., & Jamaati, R. (2022). Development and characterization of in-situ AA2024–Al_3NiCu composites. *International Journal of Metalcasting, 17*(1), 1–15. https://doi.org/10.1007/s40962-021-00752-y

Farajollahi, R., Jamshidi Aval, H., & Jamaati, R. (2022). Evaluating the microstructure, texture, and mechanical properties of AA2024–Al_3NiCu composites fabricated by the stir casting process. *CIRP Journal of Manufacturing Science and Technology, 37*, 204–218. https://doi.org/10.1016/j.cirpj.2022.01.004

Liu, C., Li, J., Zhang, W., & Pan, F. (2020). Influence of SiC addition and processing parameters on Al7075-based composites. *Journal of Materials Science & Technology, 45*, 12–20. https://doi.org/10.1016/j.jmst.2019.07.046

Onyekpe, U. J., Akande, A., & Okoro, S. C. (2022). Mechanical performance of stir-cast aluminum matrix composites for defense applications. *Defence Technology, 18*(1), 44–53. https://doi.org/10.1016/j.dt.2021.02.010

Sankar, S., Ramachandran, K. I., & Rajmohan, T. (2017). Multi-response optimization of hybrid aluminum composites using Taguchi–Grey relational analysis. *Materials Today: Proceedings, 4*(2), 2483–2492. https://doi.org/10.1016/j.matpr.2017.02.127

Sharma, S., & Chauhan, A. (2016). Optimization of tribological behavior of hybrid Al–SiC–flyash composites using Taguchi and GRA. *Procedia Materials Science, 5*, 781–790. https://doi.org/10.1016/j.mspro.2016.03.054

Singh, H., Raina, A., & Bhatt, B. (2021). Characterization and optimization of aluminum matrix composites for structural applications. *Materials Today: Proceedings, 46*(2), 8262–8266. https://doi.org/10.1016/j.matpr.2021.04.290

Zhu, Y., Chen, J., & Liu, Q. (2019). Dynamic failure mechanisms in firing pins made from different metallic materials. *Engineering Failure Analysis*, *104*, 502–510. https://doi.org/10.1016/j.engfailanal.2019.06.046